Mater. Res. Soc. Symp. Proc. Vol. 1512 © 2013 Materials Research Society
DOI: 10.1557/opl.2013.275

Real-Time Investigation of NanoFET Current Surge Capability During Heavy Ion Irradiation

Kan Xie[1], Steven Allen Hartz[1], Virginia M. Ayres[1], Zhun Liu[1], Benjamin W. Jacobs[1], Thomas Baumann[2], Reginald M. Ronningen[2], Albert F. Zeller[2], and Mary Anne Tupta[3]
[1]Department of Electrical and Computer Engineering, Michigan State University, East Lansing, MI 48824, USA
[2]National Superconducting Cyclotron Laboratory, Michigan State University, East Lansing, MI 48824, USA
[3]Keithley Instruments, Inc., Cleveland, OH 44139, USA

ABSTRACT

The real-time electronic performance of a gallium nitride nanowire-based field effect transistor was investigated at five-minute intervals over thirty minutes of continuous irradiation by Xenon-124 relativistic heavy ions. An initial current surge that resulted in device improvement rather than device failure was observed. The current surge, and subsequent electronic behavior, was modeled using a combined thermionic emission-tunnelling approach, leading to information about barrier height, carrier concentrations, expected temperature behavior, and tunnelling.

INTRODUCTION

Nanocircuits based on semiconductor nanowires, carbon nanotubes and graphene are all under intense investigation to determine how the superior electronic, thermal and mechanical properties of the component nanomaterials may translate into devices with enhanced capabilities. One situation in which electronic capability beyond state of the art is needed is in radiation environments, such as those encountered in space, particle accelerators and nuclear reactors. Research suggests that nanocircuits may offer improved tolerance and better performance [1,2]. Experiments and analyses of radiation interactions in nanocircuits are therefore needed to understand the basis for the observations and its potential for device applications.

Amongst radiation situations, those that involve heavy ions are highly destructive for current state of the art electronics [3]. Heavy ion interactions are unavoidable in space, and in many particle accelerator experiments. Nanocircuit tolerance to heavy ion irradiation would therefore represent a potentially significant application area.

In the present work, the real-time electronic performance of a gallium nitride (GaN) nanowire-based field effect transistor (nanoFET) was investigated at 5-minute intervals during 30 minutes of continuous irradiation by Xenon-124 relativistic heavy ions. As far as we know, this is the longest real-time nanowire nanoFET investigation under high-energy heavy ion irradiation to date. Threshold voltages shifts as a function of time are reported. The shifts observed immediately upon beam exposure and within the first 5-minute interval indicated a current surge. The subsequent electronic behavior from 5-30 minutes indicated the action of one or more competing mechanisms. Three models were investigated to explain the initial current surge and subsequent electronic behavior. It is shown that the experimental behavior can be successfully modeled using the combined thermionic emission-tunnelling approach, leading to information about barrier height, carrier concentrations, expected temperature behavior, and tunnelling.

EXPERIMENTAL PROCEDURES

NanoFET Fabrication

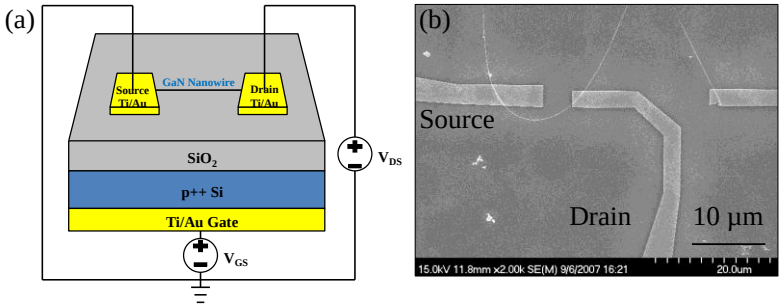

Figure 1. (a) NanoFET architecture and (b) topview SEM of EBL contacts to nanowire.

A highly doped p-type silicon wafer (~5 mΩ-cm) was used as the nanoFET substrate with a 100 nm layer of thermally grown silicon dioxide as the gate dielectric. The backside of the wafer was stripped of silicon dioxide (SiO_2) using hydrofluoric acid and Ti/Au (10/70 nm) was thermally evaporated (Edward Auto306) to form the global back gate. GaN nanowires synthesized by a catalyst-free [4] direct reaction of gallium vapor and ammonia at 850^{o}C were dispersed from an ethanol solution onto the substrate. Nanowires had a triangular profile with base widths ~60-120 nm Source and drain contacts to photo-lithographically (PL) pre-fabricated contact pads were patterned using electron beam lithography (EBL, JEOL 840A SEM). After exposure to a 100 W oxygen plasma (March Instruments PX-250) for 30 sec to remove any electron beam resist residue, Ti/Au (10/30 nm) was thermally evaporated for the conducting source and drain contacts. Subsequent metal lift-off was performed in acetone. The nanoFET architecture and a top-view SEM of the nanocircuit are shown in Figure 1 (a-b).

Real time Electronic Interface

The nanocircuit was positioned vertically in the direct beam path by replacing the scintillator plate with a custom-built non-charging mounting plate with rear openings for electrical connections to the grounded dual in-line package. The source and drain PL contact pads were connected by ultrasonic wedge wire bonding (West Bond 7400B) to the individual pins of a dual in-line package. A robotic arm with computer-driven control and laser alignment was used to center the nanocircuit within the beam path. The 96.50 mm^2 Xenon-124 beam spot size uniformly irradiated the entire active nanocircuit area. Remote connections between the vault and a control room enabled real-time electronic control, data recording and video viewing.

Beam Parameters

The experiments were performed at the National Superconducting Cyclotron Laboratory using a Xenon-124 primary beam. The Xenon-124 53+ beam with energy of 140 MeV/nucleon was focused to uniformly irradiate a 10 mm x 10 mm area (actual: 96.50 mm^2) measured from known dimensional markings on a beam-viewing scintillator plate prior to the experiments. After passing through a 0.075 mm zirconium (Zr) foil exit window and a 485 mm air gap, the beam-on-target energy was 127.33 MeV/u and the beam-on-target charge state was determined to be 75% 54+ (fully stripped), 23% 53+, and 2% 50-52+, calculated by GLOBAL [5].The ion flux was 2.95 x 10^8 ions/(cm^2 sec). The beam was blocked at 31:09 min:sec,

EXPERIMENTAL RESULTS

Real-Time Changes in I-V Characteristic During Continuous Irradiation

The nanoFET consistently reproduced the nonlinear I-V characteristic marked "pre-rad" in Figure 2 (a) during pre-radiation testing over a drain-source V_{DS} range: ±4.5 V. Families of curves, collected under gate-source (GS) bias conditions: -1.0, 0.0, +1.0 V, indicated n-type conduction. Tens of μAmps of drain-source (DS) current I_{DS} were readily obtained. The high current densities are consistent with previously reported results for GaN nanoFET devices [6].

Compliance for the real-time experiments was set to a low 1.0 μAmp to minimize electrical stress during the full 30-min experiment duration. Compliance was reached at about at V_{DS} ~ ±1.5 V. Families of curves V_{GS} curves -1.0, 0.0, +1.0 V were collected during the real-time measurements with a collection time of about 30 sec per family. V_{GS} bias voltage values were also kept low to minimize electrical stress. Only minor variations in the I-V curves were observed and therefore only the V_{GS} = + 1.0 V results are reported here.

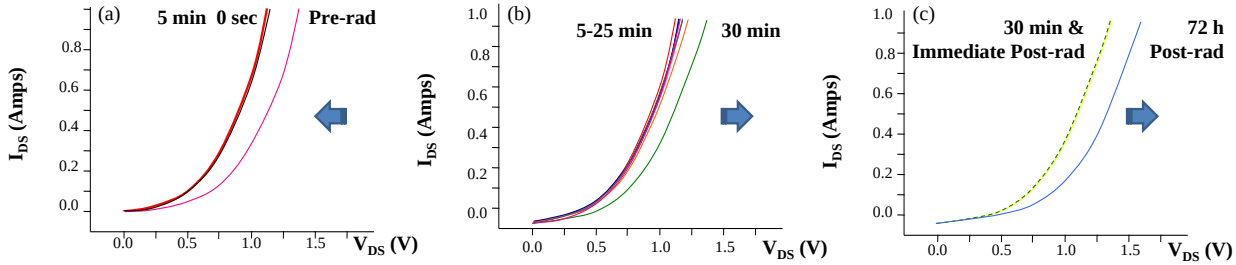

Figure 2. I-V characteristic shifts as a function of time.

During the real-time experiments, the I-V characteristic shifted to the left (lower turn-on threshold) immediately upon exposure (0 sec) to the heavy ion beam, as shown in Figure 2 (a). The leftward shift continued, with the lowest turn-on threshold observed for the 5 min measurement. After that, the I-V characteristic shifted to the right in small increments for the 10 to 25 min measurements, with a larger increase between the 25 and 30 min measurements, as shown in Figure 2 (b). The immediate post-radiation I-V characteristic showed no apparent changes. A second I-V characteristic measured at 72 h post-radiation showed a further shift to the right, as shown in Figure 2 (c).

Three models were investigated to interpret the experimental results: the space charge limited model, the thermionic emission model and the thermionic field-emission model.

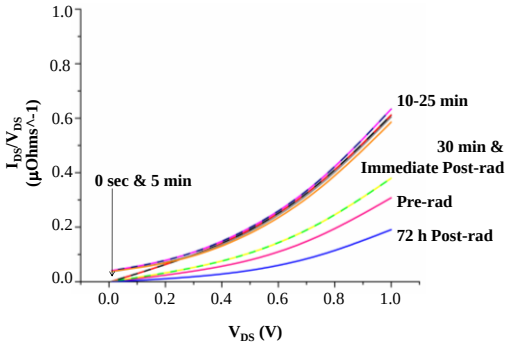

Figure 3. Nonlinear relationships between I_{DS}/V_{DS} versus V_{DS} observed for all data sets.

Interpretation by Space Charge Limited Model

Graphs of I_{DS}/V_{DS} versus V_{DS} were first investigated as a linear result indicates space charge limited (SCL) current transport in the velocity saturation regime [7]. SCL transport has been previously reported for GaN nanorod two-point measurements [8]. However, all I_{DS}/V_{DS} versus

V_{DS} plots were also nonlinear as shown in Figure 3. This suggests that the observed nonlinear I-V characteristic results from a Schottky barrier rather than SCL transport.

Interpretation by Thermionic Emission Model

The forward current data was then fit exponentially using $I_{DS} = A\exp^{BV_{DS}}$ and interpreted using a thermionic emission model [7]

$$J = \frac{I}{Area} = J_{TE}(\exp^{\frac{qV_{DS}}{nkT}} - 1) \quad (1)$$

where

$$J_{TE} = A^{*}T^{2}\exp^{\frac{-q\phi_{Bn}}{kT}} \quad (2)$$

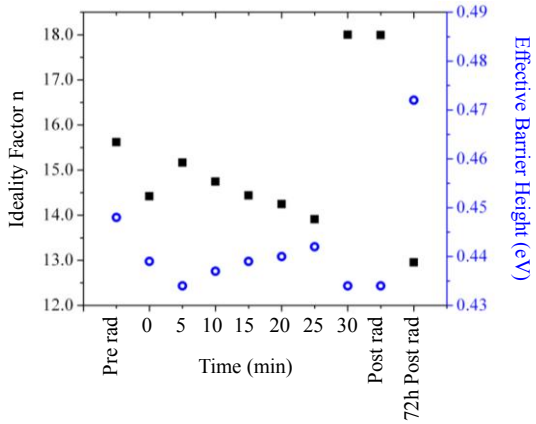

Figure 4. Ideality factors and scaled barrier heights from thermionic emission model.

A* is the Richardson constant = 120 A/cm^2 K^2, T = 300 K was assumed. A diode ideality factor n was extracted from fitting parameter B and a scaled barrier height was extracted from fitting parameter A. These are shown plotted together as a function of irradiation time in Figure 4. Ideality factor values ranged from about 13 to 18 with corresponding increases/decreases in effective barrier height. While these results are consistent with values reported for GaN nanowire devices [9], typically interpreted as indicative of tunneling, the thermionic emission model does not accommodate tunneling. When tunnelling is a significant factor, it is correct to use the combined thermionic field emission.

Interpretation by Combined Thermionic Field Emission Model

Thermionic field emission current includes tunnelling of thermally excited carriers that see a thinner barrier. A criterion for thermionic emission versus thermionic field emission versus tunneling is found by comparing the thermal energy kT to E_{00} defined as:

$$E_{00} \equiv \frac{q\hbar}{2}\sqrt{\frac{N}{m^{*}\mathcal{E}_{s}}} \quad (3)$$

For thermionic emission kT >> E_{00}, for thermionic field emission kT ~ E_{00} and for tunnelling kT << E_{00}. GaN nanowires are intrinsically n-type with a reported N range [10] of $10^{18\text{-}19}$ cm^{-3} or greater. It is simple to calculate that for N = $10^{18\text{-}19}$ cm^{-3}, $E_{00\text{-wurtzite-GaN}}$ = 0.0138-0.0438 eV and $E_{00\text{-zinc-blende-GaN}}$ = 0.0165-0.052 eV. These values are all ~ kT = 0.0259 eV, which indicates that use of the combined thermionic field emission model is correct.

$$J_{TFE} = \frac{A^{**}T\sqrt{\pi E_{00}q(\emptyset_{Bn} - \emptyset_{n} - V_{F})}}{k\cosh(E_{00}/kT)}\, exp\left[\frac{-q\emptyset_{n}}{kT} - \frac{q(\emptyset_{Bn} - \emptyset_{n})}{E_{0}}\right]\exp\left(\frac{qV_{F}}{E_{0}}\right) \quad (4)$$

where A** is the reduced effective Richardson constant that includes tunneling and also reflections at the barrier [7]. The square root factor relates the barrier height with image charge reduction to experimentally observed device operation thresholds. For the present nanoFET, this indicated that $q\phi_{Bn} - q\phi_n$ was ≥ 1.5 eV. The following factors: N, T, A** and electron energy $q\phi_n$ are all potentially significant. In this work, each of these factors was varied over an experimentally-identified range and the effect in shifting J_{TFE} to the left or to the right was investigated.

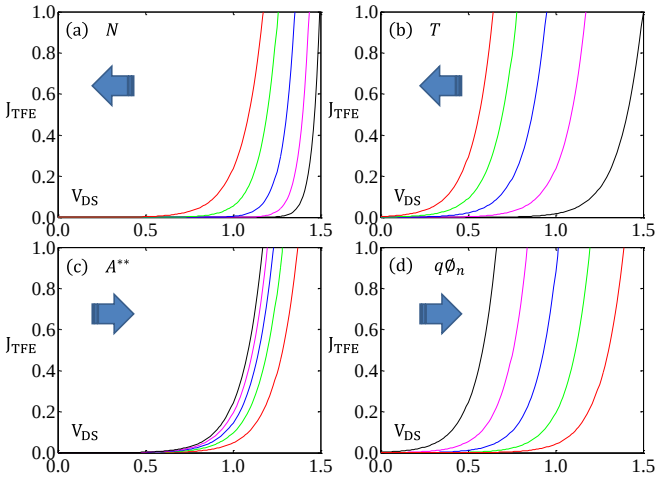

Figure 5. J_{TFE} shifts for (a) concentration N, (b) temperature T, (c) reduced effective Richardson constant A**, and (d) electron energy $q\varphi_n$.

Concentration N was varied from $10^{19\text{-}20}$ cm^{-3} in $10^{19+n \times 0.25}$ cm^{-3} increments. The remaining parameters were set as follows: $q\phi_{Bn} = 2.0$ eV and $q\phi_n = 0.2$ eV, consistent with experimental operation; T = 300 K; and A** = 14.7 A cm^{-2} K^{-1}, experimentally determined for Au on GaN [11]. The result shown black to red in Figure 5 (a) indicates that increasing N reproduces the observed initial characteristic shift to the left.

Investigation of increasing temperature was carefully studied to determine if this could account for the subsequent characteristic shift to the right. Temperature T was varied from 250-450 K in 50 K increments. Other parameters were set as before with the addition of N = 10^{20} cm^{-3}, representing the strongest current surge observed at t = 5 minutes. However, the result shown black to red in Figure 5 (b) indicates that increasing T would continue to shift the characteristic to the left. This is not consistent with the observed 10-30 minute behavior and it suggests that T did not vary greatly from 300 K during the experiment.

Tunneling can reduce the effective Richardson constant A**, e.g. from 120 to 14.7 A cm^{-2} K^{-1}. A** was varied from 15.0 *down* to 3.0 cm^{-2} K^{-1} in increments of 3.0 A cm^{-2} K^{-1}, shown black to red in Figure 5 (c). Other parameters were set as before with the addition of T = 300 K. Decreasing A** shifted the characteristic to the right. This is consistent with the experimental results for the 10-30 minute period. The further post-radiation shift might be more likely to be due to an increased barrier height as the ion-damaged surface states reset the Schottky barrier with changes to the square root factor.

Increasing the electron energy $q\phi_n$ would enable electrons to "perceive" a thinner Schottky barrier and would also facilitate tunneling. Electron energy $q\phi_n$ was varied from 0.05 to 0.25 eV in 0.05 eV increments. Other parameters were set as before with the addition of A** = 12.0 A cm^{-2} K^{-1}. Increasing $q\phi_n$ also shifted the characteristic to the right, consistent with the experimental results for the 10-30 minute period, as shown in Figure 5 (d).

DISCUSSION

In the present work, the real-time electronic performance of a GaN nanowire-based field nanoFET was investigated at 5-minute intervals during 30 minutes of continuous irradiation by Xenon-124 relativistic heavy ions. As far as we know, this is the longest real-time nanoFET investigation under high-energy heavy ion irradiation to date.

Threshold voltage shifts as a function of time were observed during real-time irradiation. The observed shifts were successfully interpreted using the thermionic-field emission model. Increasing the concentration N and the temperature T both shifted the characteristic to the left. The theoretical shift left agrees with the observed initial shift and is consistent with an initial current surge interpretation. The lack of agreement between theoretical shift left for increasing temperatures and the observed shift right as a function of time suggests that the temperature did not increase greatly during the experiment. The decreases in the effective Richardson constant and increases in the electron energy both reproduce the observed shift right. This suggests that tunneling and hot electron effects were both significant over time. Further investigation of physical factors such as dielectric changing that could influence barrier width and ion-nanowire interactions that could influence carrier energy are ongoing and will be reported in future.

CONCLUSIONS

The real-time electronic performance of a GaN nanowire-based field nanoFET was investigated at 5-minute intervals during 30 minutes of continuous irradiation by Xenon-124 relativistic heavy ions. Threshold voltage shifts as a function of time were observed during real-time irradiation and successfully interpreted using the thermionic-field emission model.

REFERENCES

1. V. M. Ayres, B. W. Jacobs, M. E. Englund, E. H. Carey, M. A. Crimp, R. M. Ronningen, A. F. Zeller, J. B. Halpern, M. Q. He, G. L. Harris, D. Liu, H. C. Shaw, M. P. Petkov, *Diamond and Relat. Mater.* **15**, 1117 (2006).
2. M.P. Petkov, L.D. Bell, H.A. Atwater, *IEEE Trans. Nucl. Sci.* **51**, 3822 (2004).
3. C. Kamezawa, H. Sindou, T. Hirao, H. Ohyama, S. Kuboyama, *Physica B* **376**, 362 (2006).
4. M. He, P. Zhou, S. N. Mohammad, G. L. Harris, J. B. Halpern, R. Jacobs, W. L. Sarney, L. J. Salamanca-Riba, *J. Cryst. Growth* **231**, 357 (2001).
5. C. Scheidenberger, T. Stohlker, W. E. Meyerhof, H. Geissel, P. H. Mokler, B. Blank, *Nucl. Instr. Meth. Phys. B* **142**, 441 (1998).
6. B. W. Jacobs, V. M. Ayres, R. E. Stallcup, A. Hartman, M. A. Tupta, A. D. Baczewski, M. A. Crimp, J. B. Halpern, M. He, H. C. Shaw, *Nanotech.* **18**, 475710 (2007).
7. S.M. Sze, K.N. Kwok, Physics of Semiconductor Devices, ISBN 978-0-471-14323-9
8. A. A.Teflin, F. Léonard, B. S. Swartzentruber, X. Wang, S. D. Hersee, Phys. Rev Lett. **101**, 076802 (2008).
9. J. R. Kim, H. Oh, H.M. So, J. J.Kim, J. Kim, C J. Lee, S. C. Lyu, *Nanotech.* **13**, 701 (2002).
10. Y. Huang, X. Duan, Y. Cui, C.M. Lieber, *Nano Lett.* **2**,101 (2002).
11. A.C. Schmitz, A.T. Ping, M. Asif Khan, Q. Chen, J.W. Yang, I. Adesida, *Semicond. Sci. Technol.* **11**, 1464 (1996).